ELSEVIER

Relict olivine, chondrule recycling, and the evolution of nebular oxygen reservoirs

A. Ruzicka [a,*], H. Hiyagon [b], M. Hutson [a], C. Floss [c]

[a] *Cascadia Meteorite Laboratory, Portland State University, Department of Geology, 17 Cramer Hall, 1721 SW Broadway, Portland, Oregon, 97207-0751, USA*
[b] *Department of Earth and Planetary Physics, The University of Tokyo, 11–16, Yaoi 2-chome, Tokyo 113, Japan*
[c] *Washington University, Laboratory for Space Sciences, Campus Box 1105, St. Louis, Missouri, 63130, USA*

Abstract

Chondrules often contain relict olivine grains that did not crystallize in situ, providing opportunities to decipher how chondrule components evolved. We studied olivine in the Sahara-97210 (LL3.2), Wells (LL3.3) and Chainpur (LL3.4) chondrites using SEM, EMPA, and SIMS techniques. Oxygen isotopes were analyzed in 16 objects from all three meteorites, and trace elements were analyzed in Sahara-97210 and Chainpur. Two groups of olivine are identified based on oxygen isotope compositions. One group is enriched in ^{16}O ($\Delta^{17}O \sim -8$ to $-4‰$) and falls close to the CCAM mixing line; it includes forsterite and Mg-rich olivine present as relict grains in Type II (ferrous) chondrules and the forsteritic cores of some isolated grains. These low-$\Delta^{17}O$ grains are poor in MnO (< 0.2 wt.%) and are usually enriched in CaO (~ 0.3–0.65 wt.%). The other group is less enriched in ^{16}O ($\Delta^{17}O \sim -3$ to $+4$ ‰); it includes normal (non-relict) ferrous olivine in type II chondrules, normal (non-relict) Mg-rich olivine in Type I (magnesian) chondrules, dusty olivine relict grains in Type I chondrules, and Mg-rich olivine relicts in a Type II and a Type I chondrule. These high-$\Delta^{17}O$ grains have variable CaO (0–0.95 wt.%) and MnO (~ 0–0.45 wt.%) contents, with the more calcic and Mn-poor compositions associated with forsteritic olivine. Trace-element data show that forsteritic olivine grains in both oxygen groups are similarly enriched in refractory elements (Al, Sc, Y, Ca, Ti, V) and depleted in volatile elements (Cr, Mn, P, Rb, sometimes K and Na) compared to normal ferrous olivine, suggesting that variations in chemical composition reflect the extent of thermal processing (greater for magnesian olivine). The data are consistent with a model in which nebular reservoirs became less enriched in ^{16}O with time. An earlier episode of chondrule formation produced Type I chondrules and isolated forsterites in carbonaceous chondrites, and forsteritic grains that were incorporated into ordinary chondrites as relict grains in chondrules and as isolated grains. Later episodes of chondrule formation produced both Type I and Type II chondrules in ordinary chondrites under a variety of thermal and redox conditions.

1. Introduction

Chondrules formed by melting at high temperatures of relatively coarse (chondrule-like) precursors, followed by rapid cooling as free-floating objects in the

* Corresponding author. Tel.: +1 503 725 3372; fax: +1 503 725 3025.

E-mail address: ruzickaa@pdx.edu (A. Ruzicka).

solar nebula [1–4]. Two major chondrule types are present in ordinary and carbonaceous chondrites, Type I (low-FeO, $Fa_{<10}$, metal-bearing), and Type II (high-FeO, $Fa_{>10}$, metal-poor) [3–6]. Type I chondrules predominate in carbonaceous chondrites, comprising >95% of all chondrules in CO, CV, CR and CM chondrites [5,7], whereas Type II chondrules predominate in H, L, and LL chondrites [3]. Despite similarities in textures and compositions, the bulk oxygen-isotope compositions of ferromagnesian chondrules in these two classes do not overlap, with those in carbonaceous chondrites being enriched in ^{16}O [4,8–10].

Variations in the bulk oxygen-isotope compositions of chondrules in carbonaceous chondrites and of their chief mineral, olivine, lie approximately on a ^{16}O-mixing line that generally overlaps the compositions of minerals found in refractory inclusions (CAIs) [8,10–15]; this mixing line is called the CCAM (carbonaceous-chondrite–anhydrous-minerals) line [16]. The variations require a mass-independent fractionation whereby chondrules in carbonaceous chondrites contain on average less of a ^{16}O-rich component than CAIs. Based on data for CAIs and chondrules in carbonaceous chondrites, including differences in composition between primary and secondary minerals, between central and enclosing objects, and differences in radiometric dates, it seems that oxygen reservoirs in the nebula evolved along the CCAM line to heavier isotopic compositions, with the production first of CAIs and then chondrules in carbonaceous chondrites [9,10,14,17,18]. Ferromagnesian and Al-rich chondrules in ordinary chondrites also require mass-independent oxygen fractionation [8,10,19,20], possibly also evolving to less ^{16}O-rich compositions [10,19–21]. The same temporal shift has been inferred based on the ^{16}O-poor compositions of magnetite grains in carbonaceous and ordinary chondrites, which are believed to have formed as late-stage secondary products [22,23]. As the O-isotope compositions of chondrules in ordinary chondrites are less enriched in ^{16}O and lie approximately on an extension of a proposed ^{16}O-mixing line for unaltered minerals in CAIs and other primary components in carbonaceous chondrites [24], this could be interpreted to indicate later formation of chondrules in ordinary chondrites than CAIs and chondrules in carbonaceous chondrites, in a system that was progressively changing in oxygen-isotopic composition from ^{16}O-rich to ^{16}O-poor.

Many chondrules were thermally reprocessed (remelted or recycled) multiple times, and contain relict grains (mostly of olivine) that were incompletely melted during the last episode of chondrule formation [4,25].

These relict grains include dusty-olivine relict grains, formed by FeO-reduction of olivine and exsolution of fine-grained metal [26–30], and Mg-olivine relict grains (which include, but are not limited to, forsterite, which we define as $Fo_{99–100}$ olivine), which probably crystallized from melts more magnesian than other host (non-relict "normal") grains in the same chondrules [4,15,25,28,31–33]. As relict grains formed before normal olivine grains, they provide an opportunity to understand chondrule evolution. In carbonaceous chondrites, it has been suggested that Type II formed after Type I chondrules, based in part on oxygen analyses of Mg-olivine relict grains in Type II ferrous chondrules [11,14,15,34].

The same type of approach for chondrules in ordinary chondrites can be used to understand the relationship between Type I and II chondrules in this class of meteorites, and to explore relationships between chondrules in ordinary and carbonaceous chondrites. In particular, the oxygen-isotope compositions of relict and normal olivine grains in chondrules from ordinary chondrites can be used to test the idea that oxygen reservoirs in the formation regions of chondrules in ordinary chondrites evolved to heavier isotopic values with time, and that some of these reservoirs could have been the same as for olivine grains in carbonaceous chondrites. Previous work has shown that some olivine grains in chondrules from various ordinary chondrites are ^{16}O-enriched similar to those in chondrules from carbonaceous chondrites [33,35,68], whereas olivine grains from other chondrules are not [23,33,35,36,68], making relationships unclear.
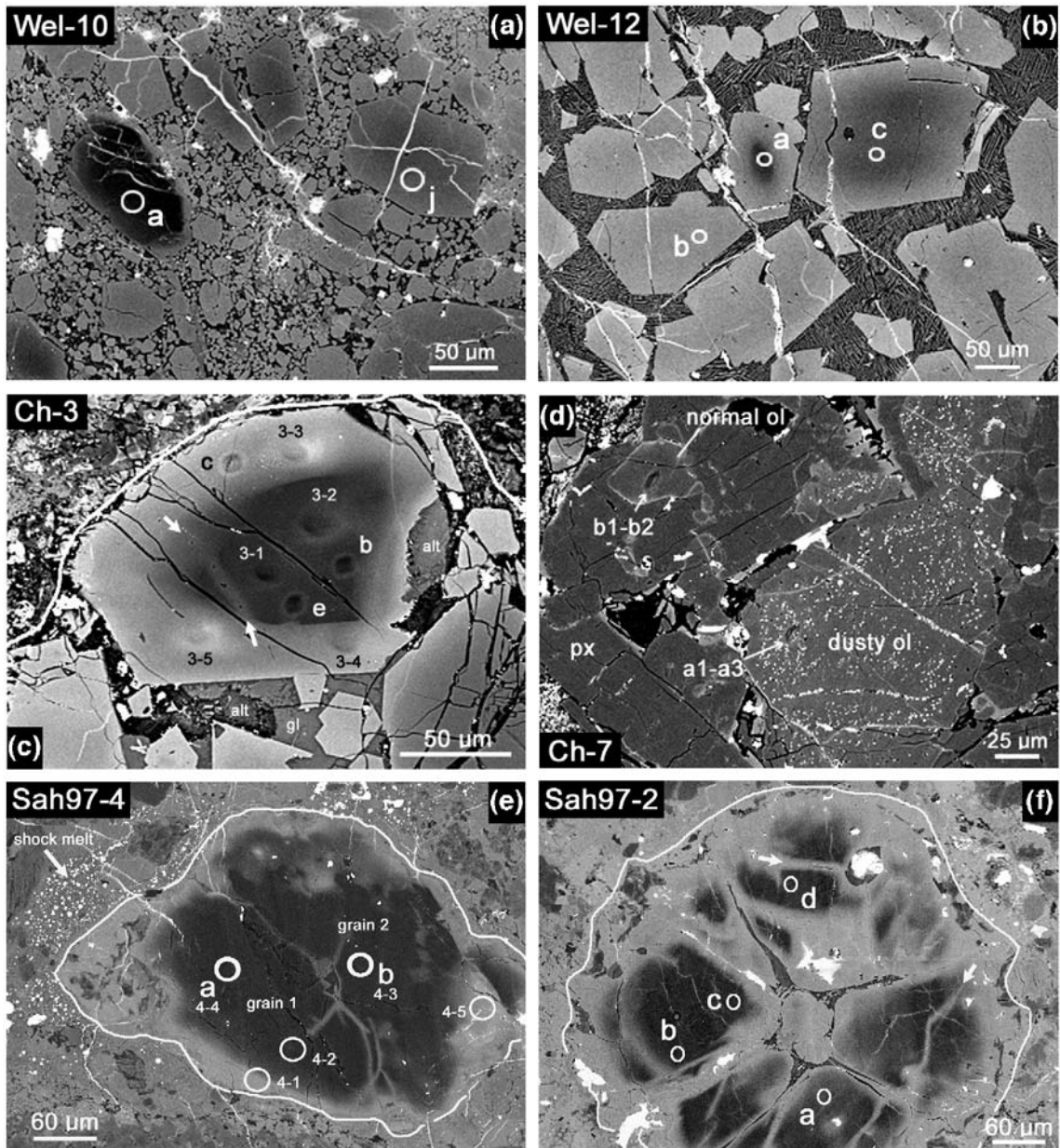
For this study, petrographic and in situ microchemical and oxygen isotope analyses were performed for olivine in three LL3 chondrites of low subtype, including Sahara-97210 (LL3.2), Wells (LL3.3), and Chainpur (LL3.4) (class and subtypes are from Koblitz [37] and the Meteoritical Society Database [69]). We also analyzed trace elements in olivine in these and other low-subtype ordinary chondrites as part of a larger study on relict grains. Sahara-97210 is minimally weathered (W0/1) but moderately shocked (S4) [37]; in our sample, shock-produced troilite veins and melt pockets are present. In contrast, Chainpur is minimally shocked (S1) [37] and is essentially unweathered (W0). Wells also appears to have been minimally shocked (S1), but it is the most weathered of the three meteorites (W2–W3), showing a distinct reddish stain and replacement of much metal by terrestrial weathering products. These meteorites are of such low subtype that their olivine oxygen-isotope compositions should have been minimally affected by thermal metamorphism [4],

considering the low diffusion rate of oxygen in this mineral [38]. Pre-terrestrial aqueous alteration was also minimal, although terrestrial weathering such as that which affected Wells could have potentially mass-fractionated oxygen to higher $\delta^{18}O$ and $\delta^{17}O$ values [9]. Preliminary results for oxygen isotopes [39,40] and trace elements [41–43] were reported previously.

2. Analytical methods

Relict olivine grains in one polished thin section each of Sahara-97210 (AMNH 4967-2), Wells (AMNH 4928-1), and Chainpur (AMNH 4020-1) were identified using a combination of optical microcopy, backscattered electron (BSE) imaging, and cathodoluminescence (CL) imaging. CL imaging using an SX-50 electron microprobe at the University of Tennessee was performed first to locate nearly pure forsterites, as these grains typically show cathodoluminescence [32,33,44]. This was followed by an optical survey using a petrographic microscope and a BSE imaging survey performed using a JEOL JSM-35C SEM at Portland State University, to identify other Mg-olivine relicts and dusty-olivine relict grains (none of the latter were found

in Sahara-97210). Representative grains were selected for quantitative WDS electron microprobe analysis (EMPA) using two Cameca SX-50 electron microprobes (at Oregon State University, Corvallis, and at the University of Tennessee, Knoxville), to characterize major-element and minor-element compositions of olivine and pyroxene in ∼1 µm-diameter analysis spots. For the dusty olivine grains, EMPA data reported here pertain to nearly metal-free areas within the grains. Operating conditions were a 15 keV accelerating voltage and a beam current of 20–50 nA. Well-characterized minerals and glasses were used as standards, and data were reduced using the PAP procedure. Microprobe and petrographic data were used to target subsequent SIMS analyses. Microprobe data were usually obtained at the same location as subsequent SIMS analyses, although EMPA data from adjacent areas in the same or adjacent grains were used to obtain average compositions in some cases.

Oxygen-isotope measurements in olivine were performed using a Cameca ims-6f ion microprobe at the University of Tokyo, using procedures similar to those described by Hiyagon and Hashimoto [45], which were modified from those by Hiyagon [46]. A Cs^+ primary beam of 0.11–0.16 nA current and 19.5 keV impact energy was used to generate negative secondary ions from samples. A normal-incidence electron gun was used for charge compensation of the sample. Secondary ions of $^{16}O^-$, $^{17}O^-$, $^{16}O^1H^-$, and $^{18}O^-$ were accelerated at −9.5 kV towards the detectors, energy filtered with an electrostatic analyzer using a 100 V window, mass separated, and detected with a Faraday Cup (^{16}O), and an electron multiplier (^{17}O, $^{16}O^1H$, and ^{18}O) in pulse-counting mode. Counts were obtained on each peak by peak jumping, with each analysis containing 100 cycles (10 blocks, 10 cycles). A mass-resolving power of 5000

was used, sufficient to clearly separate ^{17}O and $^{16}O^1H$ peaks, eliminating the need for any interference correction for ^{17}O. $^{17}O/^{16}O$ and $^{18}O/^{16}O$ ratios for cycles in each analysis were summed and averaged. All data were corrected for deadtime (though negligible for low intensities of ^{17}O and ^{18}O) and for instrumental mass fractionation by analyzing a well-characterized standard (San Carlos olivine, with assumed $\delta^{17}O=2.54$ ‰, $\delta^{18}O=4.92$ ‰ and all oxygen values on the SMOW scale) in the same runs as the unknowns, using a similar count rate of $^{16}O^-$ ions on the standard and unknowns, and normalizing data to the average of the standard analysis. No correction was made for different olivine compositions, as there is little such "matrix effect" over the range of compositions we encountered [11,46−48]. Indeed, we found no matrix effect between San Carlos olivine and synthetic forsterite within experimental uncertainty (<2‰ for $^{18}O/^{16}O$). Similarly, no matrix correction was made for dusty olivine grains that contained a small quantity (∼1 wt.%) of metal inclusions in the analysis volume. Reported uncertainties for unknowns are based on internal measurement precision. Analyses of the standard suggest a 1σ reproducibility of ∼2‰ for both $\delta^{17}O$ and $\delta^{18}O$ and ∼1‰ for $\Delta^{17}O$, similar to the uncertainties due to counting statistics alone. Analyses of unknowns were rejected if they showed a large contribution of $^{16}O^1H$ on the tail of the ^{17}O peak or large variations in the secondary beam intensity during analysis. After each run, analysis locations and craters on unknowns were documented using a JEOL-5310 SEM (BSE and secondary electron imaging) at the University of Tokyo. Analysis spots on samples were typically round or elongate and ∼15 µm in diameter.

Concentrations of trace elements in olivine were determined using the modified Cameca ims-3f ion

Fig. 1. BSE images of objects in Wells (Wel), Chainpur (Ch), and Sahara-97210 (Sah97). (a) Chondrule Wel-10 has euhedral olivine set in a glassy mesostasis; the crater locations of O-analysis sites 'a' (in a Mg-olivine relict grain) and 'j' (normal grain) are indicated. Bright veins are filled with terrestrial weathering products. (b) Chondrule Wel-12 has euhedral olivine set in a mesostasis of glass and fine-grained pyroxene crystallites; the crater locations of O-analysis sites 'a' (relict Mg-olivine core of grain), 'b' (normal grain), and 'c' (anomalously magnesian and possibly relict grain) are indicated. Bright veins are filled with terrestrial weathering products. (c) Chondrule Ch-3 (edge indicated by white line) contains a prominent forsterite relict grain core (dark grey) surrounded by a ferrous overgrowth (light grey); SIMS crater pits for O-analyses ('b', 'c', 'e') and trace-element analyses (3-1, 3-2, 3-2, 3-4) are visible. A veinlet of pitted ferrous olivine cross-cuts the relict core (arrows). Minor replacement of chondrule glass (gl) and overgrowth olivine with alteration products (alt) has occurred probably as a result of aqueous alteration on the parent body. (d) Chondrule Ch-7 contains a large dusty-olivine relict (dusty ol) and normal olivine (normal ol), low-Ca pyroxene (px), and minor feldspathic glass; two crater pits for O-analyses in the dusty relict (analyses a1, a2, a3, taken in the same location) and normal olivine (b1, b2, same location) are visible. (e) Object Sah97-4 (shown with outline) is composed of two attached forsterite grains (dark grey) separated by a thin Fe-olivine overgrowth (bright line from upper left to lower right) and a glass patch; the two grains are surrounded in turn by a ferrous olivine overgrowth (light grey) and some feldspathic material. SIMS O-isotope ('a', 'b') and trace element (4-1, 4-2, 4-3, 4-4, 4-5) crater locations are indicated. Shock melt is located just outside the object at upper left, and shock-produced troilite veins (bright features) extend into it. A portion of the object has been microfaulted at right (adjacent to trace-element spot 4-5). Along this microfault, forsterite abuts directly against ferrous overgrowth with no discernible Fe–Mg exchange, implying minimal post-shock chemical diffusion in Sahara-97210. (f) Chondrule Sah97-2 is composed chiefly of forsterite grains (dark grey) that have prominent ferrous olivine overgrowths (light grey) and veinlets (arrows); metal (bright) and glass inclusions occur in some olivine grains (e.g., at upper right), and glassy mesostasis separates the olivine grains. The locations of O-analysis craters ('a', 'b', 'c', 'd') are indicated.

Table 1
Petrographic and olivine data for objects in Wells (Wel), Chainpur (Ch), and Sahara-97210 (Sah97)

Object	Type [a]	Texture and mineralogy [b]	Diameter [c]	Normal olivine grains [d]	Relict olivine grains [d]
Wel-2	IA	PO; ol, gl, px, met	520	Fo_{97-100} cores/Fo_{89-97} rims	None
Wel-4	IIAB	POP; ol, px, gl, cpx, neph	775	Fo_{68-80}	$Fo_{97-99.6}$ core/Fo_{65-80} ovg.
Wel-10	IIA	PO; ol, gl, crystallites	650×790	Fo_{69-85}	(1) Fo_{91-98} core/Fo_{68-78} ovg.
					(2) Fo_{95-96} core/Fo_{70-79} ovg.
Wel-12	IIA	PO; ol, px, gl	1640×2130	Fo_{65-84}	Fo_{76-90} small core/Fo_{69-82} ovg.
Ch-1	IIA	PO; ol, gl, crystallites, partial troi rim	630	Fo_{72-84}	(1) $Fo_{99.3}$ small core/Fo_{75-86} ovg.
					(2) Fo_{92-93} core/Fo_{69-71} ovg.
Ch-3	IIA	PO; ol, gl, crystallites	410×470	Fo_{63-86}	$Fo_{99.2-99.8}$ core/Fo_{69-83} ovg.
Ch-7	IAB	POP; px, ol, gl, met, troi, partial troi rim	570	Fo_{87-96}	Fo_{89-93} dusty
Ch-8	IIAB	POP; ol, px, feld, cpx	520×650	Fo_{62-71}	Fo_{95} core/Fo_{65-67} ovg.
Ch-9	IAB	POP; px, ol, gl, met, cpx, fine-grained troi-rich rim	640	Fo_{95-97}	Fo_{89-94} dusty
Sah97-2	IA	PO; ol, gl, met, px, minor troi veins	450	$Fo_{98-99.5}$ cores/Fo_{65-84} ovg.	None, or forsteritic cores
Sah97-4	IA or IOG	2 ol grains with intervening gl; met, minor troi veins	290×390	$Fo_{97-99.5}$ cores/Fo_{55-85} ovg.	None, or forsteritic cores
Sah97-5	IA	BO; ol, gl, px rim	550×590	Fo_{71-97}	$Fo_{98-99.4}$ core/Fo_{71-98} rim
Sah97-7	IA	PO; ol, gl, troi (shock melt), px rim, met	~1300	Fo_{69-98}	$Fo_{98-99.3}$ core/Fo_{81-91} ovg.
Sah97-8	IA or IOG	ol grain with attached gl, crystallites	165×190	$Fo_{98-99.4}$ core/Fo_{63-97} ovg.	None, or forsteritic core
Sah97-9	Al-rich	PO; ol, gl, fas	170×310	$Fo_{98-99.6}$ core/Fo_{68-91} ovg.	None, or forsteritic core
Sah97-10	IA?	Non-porphyritic ol, px rim, troi, met, gl	370×530	$Fo_{98-99.1}$ cores/Fo_{69-98} other	None, or forsteritic cores

[a] I = low-FeO chondrule, II = high-FeO chondrule, A = olivine-rich, AB = olivine and pyroxene-rich, IOG = isolated olivine grain.

[b] Textures: PO = microporphyritic olivine; POP = microporphyritic olivine-pyroxene; BO = barred olivine. Mineralogy: listed in approximate decreasing abundance in each object; ol = olivine, px = low-Ca pyroxene, cpx = pigeonite or augite, gl = glass, met = Fe-metal alloy, troi = troilite, fas = fassaite, neph = nepheline, feld = feldspar.

[c] Approximate diameter (μm) in thin-section.

[d] ovg. = overgrowth. $Fo = 100 \times Mg/(Mg+Fe)$ atomic.

microprobe at Washington University, according to techniques described by Zinner and Crozaz [49]. All analyses were made using an O^- primary beam and energy filtering at low mass resolution to remove complex molecular interferences. The resulting mass spectrum is deconvolved in the mass ranges K–Ca–Sc–Ti and Rb–Sr–Y–Zr to remove simple molecular interferences that are not eliminated with energy filtering [50,51]. Sensitivity factors for the REE are from Zinner and Crozaz [52], and those for other elements are from Hsu [50]. Absolute concentrations are determined by normalizing the ion signals relative to Si, using SiO_2 concentrations determined by electron microprobe analyses of the specific grains chosen for ion probe analysis, and errors are due to counting statistics only. After trace-element runs, analysis locations were documented by optical petrography and with the SEM at Portland State University.

3. Results

3.1. Wells

Oxygen-isotope data were obtained for olivine grains in microporphyritic olivine (PO) chondrules in Wells, including one typical Type I chondrule with no obvious relict grains and three Type II chondrules with obvious relict Mg-olivine grains (Fig. 1a,b; Tables 1 and 2). All olivine grains analyzed in Wells have $\delta^{18}O$ values less than the ordinary chondrite bulk chondrule field (Fig. 2). This is unlike what one would expect for terrestrial weathering, assuming that the bulk chondrule field represents the composition of typical unweathered material in ordinary chondrites. Deviations in ^{17}O from the terrestrial mass fractionation (TF) line are summarized by $\Delta^{17}O = \delta^{17}O - 0.52 \times \delta^{18}O$, and most grains in Wells have $\Delta^{17}O \sim 0 \pm 3$‰ (Table 2) and overlap the TF line (Fig. 2). These same grains have variable Fo contents, ranging from $Fo_{71-99.2}$ (Table 2). They include all of the ferrous olivine grains from Type II chondrules, magnesian grains in the Type I chondrule, and two obvious Mg-olivine relict grains in Wel-10 (Figs. 1a and 2). However, two Mg-olivine relict grains have oxygen-isotope compositions that lie well off the TF line, with $\Delta^{17}O \sim -6$ to -8 ‰; they plot close to the CCAM and proposed primordial slope=1 mixing lines (Fig. 2). They include in Wel-4 a $\sim 50 \times 100$ μm-diameter Fo_{99} relict grain core surrounded by a ~ 20 μm wide ferrous overgrowth, and in Wel-12 a $\sim 26 \times 37$ μm-diameter relict grain core (as magnesian as Fo_{90}) surrounded by a $\sim 30-70$ μm wide ferrous overgrowth (Fig. 1b). These grains are clearly out of isotopic equilibrium with other

olivine grains in the host chondrules. For Wells, there is no simple relationship between O-isotopic compositions with either Fo content or grain type (relict or normal), although the only grains that clearly lie off the TF line are relict.

3.2. Chainpur

Three Type II PO chondrules with obvious Mg-olivine relict grains and two Type I POP chondrules with dusty-olivine relict grains were analyzed for oxygen isotopes in Chainpur (Fig. 1c,d; Tables 1 and 2). For the PO chondrules, normal olivine grains plot close to the TF line, but at lower $\delta^{18}O$ and $\delta^{17}O$ values than the ordinary chondrite bulk chondrule field (Fig. 3a). The isotopic compositions of relict Mg-olivine grains analyzed in these chondrules have obvious enrichments in ^{16}O ($\Delta^{17}O$ as low as $\sim -8‰$) compared to normal ferrous olivine grains in the same chondrules, and plot close to the CCAM and slope = 1 mixing lines (Fig. 3a). These data suggest that the relict grains crystallized in an isotopically distinct reservoir that was enriched in ^{16}O compared to the host chondrules. The low-$\Delta^{17}O$ grains include a large ($\sim 105 \times 75$ μm-diameter) nearly pure forsterite ($Fo_{99.6}$) relict core surrounded by a ~ 33–40 μm wide ferrous overgrowth in Ch-3 (Fig. 1c); a $\sim 110 \times 95$ μm-diameter Mg-olivine (to Fo_{95}) relict core surrounded by a ~ 17 μm-wide ferrous overgrowth in Ch-8; and a $\sim 67 \times 40$ μm-diameter Mg-olivine (Fo_{92-93}) relict core surrounded by a ~ 10–13 μm-wide ferrous overgrowth in Ch-1. The overgrowth in Ch-3 isotopically resembles normal olivine in the same chondrule (Fig. 3a). This suggests that it crystallized from the same reservoir as the normal grains, probably in the same melting event that produced the normal grains. For the POP chondrules, dusty and normal olivine grains plot close to the TF line (Fig. 3b). Based on multiple analyses it appears that the dusty olivine relict in Ch-7 has lower $\delta^{18}O$ and $\delta^{17}O$ values than the largest normal grain in this chondrule (Fig. 3b). The dusty relict in Ch-7 is unusually coarse ($\sim 63 \times 400$ μm across) and located at the center of the chondrule (Fig. 1d). The isotopic data for both types of grains in Ch-7 roughly parallel the TF line (Fig. 3b), consistent with mass-dependent fractionation between the relict and normal grains. As with Wells, the only grains that clearly lie off the TF line are Mg-olivine relict grains.

3.3. Sahara-97210

Seven objects were analyzed for oxygen isotopes in Sahara-97210 (Tables 1 and 2, Fig. 1e,f). Two of them,

Sah97-4 (Fig. 1e) and Sah97-8, could be described as "isolated olivine" grains. All the analyzed objects are dominated by olivine grains with forsteritic cores ($Fo_{97-99.6}$) and ferrous rims or overgrowths (Fo_{55-98}), making it difficult to identify which grains are relict and which are normal but strongly zoned (Table 1). Conversely, it is possible that some of these objects (such as Sah97-2, Fig. 1f) consist of multiple relict grains, as suggested by large compositional differences between core and overgrowth portions of grains (Table 1). The "isolated" grains contain Mg-rich cores ($Fo_{97-99.5}$) surrounded by ferrous overgrowths (Fo_{55-97}), but they are actually polygranular and polycrystalline objects that contain feldspathic glass. They resemble olivine grains in some Type I chondrules such as Sah97-2 (Fig. 1f) in terms of olivine compositions and grain sizes, and in having some specific textural features, such as ferrous olivine veinlets that cross-cut forsteritic cores (Fig. 1e,f). A similar ferrous veinlet occurs in the prominent forsterite relict in Ch-3 (Fig. 1c). Thus, we interpret the "isolated grains" as fragments of Type I chondrules that contained magnesian grains. Except for the chondrule fragments, the oxygen-isotopic compositions of olivine grains in Sahara-97210 lie close to the TF line, with $\Delta^{17}O$ $\sim 0 \pm 3‰$ (Fig. 4). The fragments, Sah97-4 and Sah97-8, have ^{16}O-enriched compositions ($\Delta^{17}O$ ~ 5.5–7.1‰) that tend to be shifted to higher $\delta^{18}O$ values compared to the CCAM line (Fig. 4), but they barely overlap with the CCAM line if one considers 2σ errors. These isotopic compositions, including possible occasional shifts off the CCAM line, are similar to those reported for "isolated grains" in carbonaceous chondrites [11,47,53,54]. Many of the other objects in Sahara-97210 that lie close to the TF line also have relatively high $\delta^{18}O$ and $\delta^{17}O$ (Fig. 4). Despite the low weathering grade (W0/1), this shift is conceivably due to terrestrial weathering. It is also conceivable that shock-metamorphism, which was significant for Sahara-97210, could have affected isotopic compositions somewhat and caused an increase in $\delta^{18}O$ and $\delta^{17}O$ values.

3.4. Relationship between isotopic and chemical composition

Fig. 5 shows the relationship between chemical and isotopic composition for olivine in all objects that have some grains with $\Delta^{17}O$ distinct from the TF line (dashed), whereas Fig. 6 shows the same data for objects that have no grains with $\Delta^{17}O$ clearly distinct from the TF line. In both cases, data are taken from Table 2. Complete chemical compositions based on EMPA data are provided in an electronic data supplement

Table 2
Oxygen isotopic compositions and corresponding chemical (EMPA) data for objects in Wells (Wel), Chainpur (Ch), and Sahara-97210 (Sah97) (values in parentheses are $\pm 1\sigma$ errors, based on counting statistics for O-isotope values, and standard deviations of means for chemical data)

Object/position	$\delta^{17}O$ (‰)	$\delta^{18}O$ (‰)	$\Delta^{17}O$ (‰)	Comment[a]	Fo (at.%)	CaO (wt.%)	MnO (wt.%)
Wel-2							
a	−4.5 (2.0)	−6.7 (2.4)	−1.0 (2.0)	gr. core	99.2 (0.6)	0.43 (0.08)	0.02 (0.04)
b	−5.1 (1.9)	−8.9 (2.3)	−0.4 (1.9)	Pyroxene	Wo$_{4.5}$En$_{94.2}$		
Wel-4							
a	−12.1 (1.7)	−12.5 (2.5)	−5.7 (1.7)	Relict gr. core	99.0 (0.6)	0.40 (0.06)	<0.01
b	−4.1 (1.8)	+0.7 (2.5)	+2.4 (1.3)	Normal gr. 1 core	79.5	0.12	0.41
d	+2.8 (1.4)	−7.3 (2.5)	−0.3 (1.6)	Normal gr. 2	73.6 (0.3)	0.17 (0.01)	0.49 (0.05)
e	−1.0 (1.7)	−0.3 (2.5)	−0.8 (1.7)	Normal gr. 3	75.2 (0.4)	0.11 (0.01)	0.42 (0.05)
Wel-10							
a	−3.0 (1.7)	−5.6 (2.5)	−0.1 (1.5)	Relict gr. 1 core	96.5 (1.4)	0.95 (0.17)	0.01 (0.01)
b	−5.0 (1.6)	−8.5 (2.5)	−0.6 (1.4)	Relict gr. 2 core	95.8 (0.4)	0.18 (0.02)	0.04 (0.01)
h	−3.6 (1.6)	−5.9 (2.5)	−0.6 (1.4)	Normal gr. 1	72.2 (0.9)	0.14 (0.04)	0.46 (0.01)
J	−3.6 (1.7)	−8.4 (2.5)	+0.7 (1.5)	Normal gr. 2 core	79.2 (1.2)	0.08 (0.04)	0.34 (0.03)
K	−2.6 (1.7)	−6.4 (2.5)	+0.8 (1.6)	Normal gr. 3	73.9 (0.9)	0.18 (0.06)	0.41 (0.03)
Wel-12							
a	−14.0 (1.9)	−12.6 (2.4)	−7.5 (1.9)	Relict gr. core	85.0 (4.2)	0.33 (0.06)	0.17 (0.07)
b	+0.9 (1.9)	−1.4 (2.2)	+1.6 (1.8)	Normal gr.1	70.6 (0.9)	0.14 (0.03)	0.47 (0.04)
c	+4.1 (1.9)	+1.1 (2.3)	+3.5 (1.9)	Normal gr. 2 core	81.2 (2.4)	0.10 (0.01)	0.31 (0.02)
d	+3.0 (2.1)	+3.3 (2.3)	+1.2 (2.1)	Normal gr. 3 core	77.5 (1.0)	0.09 (0.03)	0.33 (0.03)
Ch-1							
b1	−9.1 (1.9)	−5.8 (2.3)	−6.1 (1.9)	Relict gr. 2 core	92.8 (0.5)	0.03 (0.02)	0.04 (0.01)
b2	−11.8 (1.9)	−6.8 (2.4)	−8.3 (1.9)	Relict gr. 2 core	92.8 (0.5)	0.03 (0.02)	0.04 (0.01)
a1	−0.7 (1.9)	+2.6 (2.4)	−2.1 (1.9)	Normal gr. 1 core	81.1	<0.01	0.31
a2	+2.0 (1.8)	+3.4 (2.3)	+0.2 (1.8)	Normal gr. 1 core	81.1	<0.01	0.31
c	+0.1 (1.8)	+1.1 (2.3)	−0.5 (1.8)	Normal gr. 2	72.6	0.05	0.43
Ch-3							
b	−12.7 (1.8)	−9.8 (1.5)	−7.6 (1.8)	Relict gr. core	99.7 (0.1)	0.65 (0.06)	<0.01
e	−9.0 (1.7)	−8.4 (1.7)	−4.6 (1.7)	Relict gr. core	99.7 (0.1)	0.65 (0.06)	<0.01
c	+0.5 (1.8)	+1.5 (1.5)	−0.2 (1.8)	Relict gr. ovg.	76.0 (4.4)	0.06 (0.01)	0.31 (0.04)
a	+1.1 (1.8)	−1.2 (1.5)	+1.7 (1.8)	Normal gr. 1 core	84.1 (1.5)	0.08 (0.02)	0.23 (0.04)
d	+1.8 (1.9)	+0.2 (1.5)	+1.7 (1.8)	Normal gr. 2	78.2 (0.7)	0.09 (0.02)	0.30 (0.04)
Ch-7							
a2	−0.4 (2.1)	−3.2 (2.4)	+1.2 (2.1)	Relict dusty gr.	90.9 (0.8)	<0.01	0.32 (0.09)
a3	−0.9 (1.8)	+1.3 (2.3)	−1.5 (1.8)	Relict dusty gr.	90.9 (0.8)	<0.01	0.32 (0.09)
b1	−1.7 (1.9)	−0.7 (2.3)	−1.3 (1.9)	Relict dusty gr.	90.9 (0.8)	<0.01	0.32 (0.09)
b2	+1.9 (1.9)	+4.7 (2.4)	−0.5 (2.0)	Normal gr.	92.6 (3.0)	0.08 (0.02)	0.15 (0.03)
	+2.5 (1.9)	+5.7 (2.3)	−0.5 (1.9)	Normal gr.	92.6 (3.0)	0.08 (0.02)	0.15 (0.03)
Ch-8							
a1	−4.2 (1.8)	−1.3 (2.3)	−3.5 (1.8)	Relict gr. core edge	88.0 (7.6)	0.05 (0.06)	0.14 (0.09)
a2	−6.8 (1.9)	−3.1 (2.4)	−5.2 (2.0)	Relict gr. core edge	88.0 (7.6)	0.05 (0.06)	0.14 (0.09)
b	−1.6 (1.9)	+3.1 (2.3)	−3.2 (1.8)	Normal gr. core	70.8	0.05	0.36
Ch-9							
a1	−3.4 (1.9)	−0.1 (2.3)	−3.3 (1.9)	Relict dusty gr.	92.6 (1.3)	0.02 (0.04)	0.30 (0.04)
a2	−0.1 (1.8)	+3.0 (2.3)	−1.6 (1.8)	Relict dusty gr.	92.6 (1.3)	0.02 (0.04)	0.30 (0.04)
a3	−2.4 (2.0)	−0.7 (2.3)	−2.0 (2.0)	Relict dusty gr.	92.6 (1.3)	0.02 (0.04)	0.30 (0.04)
b1	−1.2 (1.8)	+2.3 (2.3)	−2.4 (1.8)	Normal gr. core	95.6 (0.7)	0.05 (0.03)	0.23 (0.08)
b2	+0.7 (1.9)	+2.6 (2.3)	−0.7 (1.9)	Normal gr. core	95.6 (0.7)	0.05 (0.03)	0.23 (0.08)
b3	−2.8 (1.8)	+0.6 (2.3)	−3.1 (1.8)	Normal gr. core	95.6 (0.7)	0.05 (0.03)	0.23 (0.08)

Table 2 (*continued*)

Object/position	$\delta^{17}O$ (‰)	$\delta^{18}O$ (‰)	$\Delta^{17}O$ (‰)	Comment [a]	Fo (at.%)	CaO (wt.%)	MnO (wt.%)
Sah97-2							
a	+2.7 (1.7)	+9.0 (2.5)	−2.0 (1.0)	gr. 1 core	98.9 (0.3)	0.49 (0.01)	<0.01
b	+5.1 (1.8)	+10.6 (2.5)	−0.4 (1.1)	gr. 2 core	98.9 (0.6)	0.48 (0.07)	<0.01
c	+7.5 (1.8)	+14.4 (2.5)	+0.1 (1.1)	gr. 2 core	98.9 (0.6)	0.48 (0.07)	<0.01
d	+6.2 (1.8)	+13.5 (2.4)	−0.8 (1.0)	gr. 3 core	98.7 (0.3)	0.51 (0.02)	0.01 (0.01)
Sah97-4							
a	−2.6 (1.8)	+6.5 (2.5)	−5.9 (1.1)	gr. 1 core	99.3 (0.3)	0.43 (0.17)	0.01 (0.01)
b	−2.5 (1.8)	+5.8 (2.5)	−5.5 (1.0)	gr. 2 core	98.9 (0.5)	0.53 (0.04)	0.01 (0.01)
Sah97-5							
a3	+2.2 (1.9)	+0.7 (2.2)	+1.9 (1.7)	Relict gr. core	99.1 (0.3)	0.47 (0.03)	<0.01
b1	+1.6 (2.1)	+2.3 (2.3)	+0.4 (2.0)	Normal gr. 1 core	96.8 (0.4)	0.39 (0.01)	<0.01
b2	+1.7 (2.1)	+2.4 (2.3)	+0.4 (1.9)	Normal gr. 1 core	96.8 (0.4)	0.39 (0.01)	<0.01
c3	+4.2 (2.0)	+2.3 (2.2)	+3.0 (1.8)	Normal gr. 2 rim	74.7 (1.5)	0.19 (0.08)	0.32 (0.07)
Sah97-7							
a	+4.3 (1.8)	+8.7 (2.5)	−0.3 (1.0)	Normal gr. 1	92.9 (2.0)	0.26 (0.18)	0.06 (0.01)
b	+5.9 (1.8)	+11.1 (2.4)	+0.2 (1.0)	Normal gr. 2	95.5 (2.9)	0.35 (0.17)	0.01 (0.01)
c	+3.0 (1.8)	+10.1 (2.5)	−2.2 (1.0)	Normal gr. 3	97.2 (0.1)	0.44 (0.01)	0.04 (0.01)
Sah97-8							
a	−6.3 (1.8)	+1.6 (2.4)	−7.1 (1.1)	gr. core	99.0 (0.5)	0.56 (0.07)	0.01 (0.01)
b	−8.7 (1.8)	−3.9 (2.4)	−6.6 (1.0)	gr. core edge	95.2 (1.1)	0.42 (0.07)	0.03 (0.01)
Sah97-9							
a2	−1.4 (1.4)	−2.1 (1.3)	−0.3 (1.6)	gr. core	99.0 (0.5)	0.43 (0.04)	<0.01
a3	+0.7 (1.5)	−0.5 (1.1)	+0.9 (1.7)	gr. core	99.0 (0.5)	0.43 (0.04)	<0.01
b1	−0.2 (1.5)	+0.5 (1.2)	−0.4 (1.7)	ovg.	71.7 (4.2)	0.19 (0.13)	0.38 (0.08)
b2	−0.6 (1.5)	−0.1 (1.2)	−0.5 (1.8)	ovg.	71.7 (4.2)	0.19 (0.13)	0.38 (0.08)
Sah97-10							
e1	+5.2 (2.1)	+7.7 (2.2)	+1.2 (1.9)	gr. core 1	98.9 (0.1)	0.40 (0.02)	0.01 (0.01)
e2	+7.5 (2.0)	+8.3 (2.3)	+3.2 (1.8)	gr. core 1	98.9 (0.1)	0.40 (0.02)	0.01 (0.01)
e3	+5.8 (2.0)	+9.8 (2.2)	+0.8 (1.8)	gr. core 2	93.4	0.25	0.06
d2	+5.1 (2.0)	+2.3 (2.3)	+3.9 (1.8)	ovg.	70.3 (1.4)	0.06 (0.02)	0.41 (0.03)
d3	+4.5 (2.1)	+4.4 (2.3)	+2.2 (1.9)	ovg.	70.3 (1.4)	0.06 (0.02)	0.41 (0.03)

[a] gr. = grain, ovg. = overgrowth.

(Appendix 1). As objects with low $\Delta^{17}O$ are also enriched in ^{16}O (Figs. 2–4), ^{16}O is progressively depleted from left to right in Figs. 5 and 6. Fig. 5 reveals that low-$\Delta^{17}O$ grains ($\Delta^{17}O \sim -8$ to $-4‰$) are forsteritic (Fo_{85-100}), typically calcic (CaO ~ 0.3–0.65 wt.%), and MnO-poor (0–0.2 wt.%). They are chemically distinct from high-$\Delta^{17}O$ grains ($\Delta^{17}O \sim -3$ to $+4‰$) in the same objects, which are less forsteritic (Fo_{70-85}), less calcic (CaO < 0.2 wt.%), and enriched in MnO (0.2–0.5 wt.%). Thus, for this subset of objects, isotopic and chemical compositions are correlated. However, Fig. 6 shows that this is clearly not the case for the olivine grains in other objects, which have generally uniform $\Delta^{17}O$ (−3 to +4‰), but variable chemistry (Fo_{70-100}, CaO ~ 0–0.95 wt.%, MnO ~ 0–

0.45 wt.%). Moreover, even within the low-$\Delta^{17}O$ group, relict grains in Ch-8 and Wel-12 are noticeable poorer in Ca, richer in Mn, and have lower values of Fo than other grains of similar $\Delta^{17}O$ (Fig. 5). This clearly shows that for olivine there is a decoupling between chemical and isotopic compositions. Contrary to the conclusions of Pack et al. [33], it is apparent that forsterite grains are not always ^{16}O-rich. However, all ^{16}O-rich grains are relatively magnesian and usually calcic. For all of the grains we analyzed, there is also a consistent relationship whereby forsteritic grains, either in Type I chondrules or as relict Mg-olivine grains in Type II host chondrules, tend to be calcic and Mn-poor. More ferrous olivine grains in Type II chondrules, or
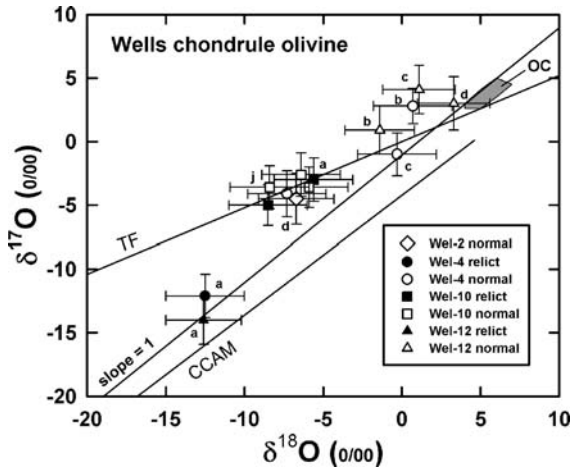
Fig. 2. Standard 3-isotope diagram for oxygen, showing the composition of olivine in Wells. Error bars are ±1σ. OC = field of bulk chondrule compositions in ordinary chondrites [9]; CCAM = carbonaceous–chondrite–anhydrous-minerals mixing line (regression line through data given in [16]); TF = terrestrial mass-fractionation line; the line labeled "slope = 1" is a proposed primordial ^{16}O-mixing line [24].

ferrous olivine present as overgrowths on forsteritic grains, tend to be Ca-poor and Mn-rich.

3.5. Chemical composition as an indicator of thermal processing

The significance of chemical variations in olivine can be best understood by utilizing SIMS trace element data for olivine. In Fig. 7, we compare the compositions of forsterites (Fo$_{99–100}$) in Sahara-97210 and Chainpur with those of normal ferrous olivine (Fo$_{70–89}$) in Chainpur. Data are shown for elements whose concentrations in olivine are not strongly affected by cooling rate during crystallization [41,42]. Appendix 2 in the data supplement has more complete trace element data. The compositions of forsterites in the two meteorites are similar, although alkalis, V, and to some extent siderophiles are enriched in the forsterites from Sahara-97210 (Fig. 7), possibly as a result of the greater shock metamorphism it experienced. Troilite shock-melt veins often extend into the Sahara-97210 objects (Fig. 1e), suggesting that the trace-element compositions of olivine grains in this meteorite could easily have been affected by shock. The enrichment in alkalis could indicate a small amount of contamination by feldspathic melt shock-injected into olivine. Despite these differences, it is apparent that the forsterite grains in both meteorites are relatively refractory and depleted in siderophiles compared to the normal olivine grains (Fig. 7). Significantly, the forsterites are enriched on

average in elements that have high 50% condensation temperatures (Al, Sc, Y, Ca, Ti, V), and depleted in elements that have low 50% condensation temperatures (Cr, Mn, P, Rb, and sometimes K and Na) (Fig. 7). This difference in trace-element composition between forsterite and ferrous olivine implies that vapor-fractionation, involving either condensation or evaporation or both, was important.

Thus, it appears that the chemical variations in olivine shown in Figs. 5 and 6 largely reflect thermal processing, with magnesian, Ca-rich, and Mn-poor grain compositions indicative of more thermal processing, and ferrous, Ca-poor, and Mn-rich grain compositions indicative of less thermal processing. This conclusion is consistent with the open-system experiments of Cohen et al. [55] on a CI chondrite analog starting composition, who found that Type I-like forsteritic and calcic olivine can be produced by longer duration evaporative heating, and
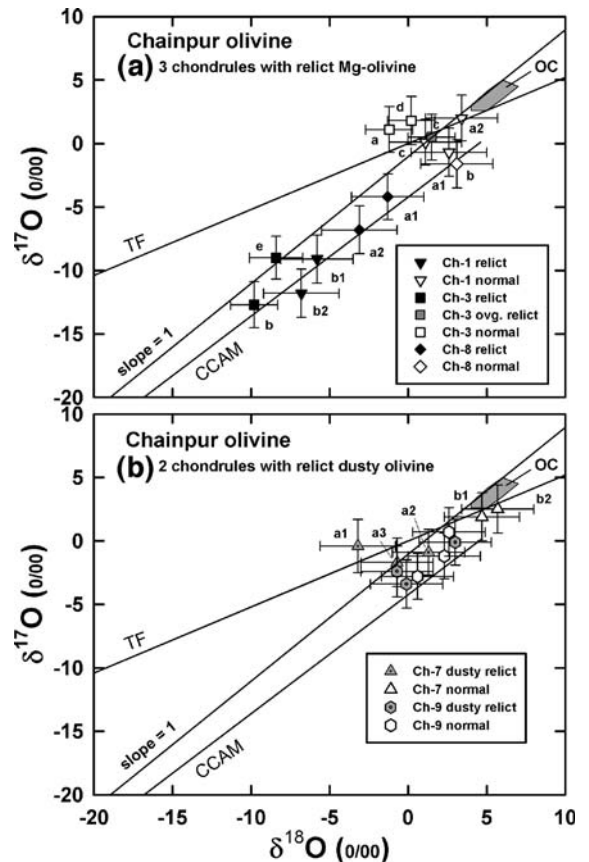

Fig. 3. Standard 3-isotope diagram for oxygen, showing the composition of olivine in Chainpur: (a) olivine in 3 microporphyritic olivine chondrules in Chainpur that contain Mg-olivine relict grains, and (b) olivine in 2 microporphyritic pyroxene-olivine chondrules in Chainpur that contain dusty-olivine relict grains. Ovg. = overgrowth; other labels are the same as in Fig. 2.

Type IIA-like ferrous and Ca-poor olivine by shorter duration heating. Alternatively, forsteritic and Ca-rich, Mn-poor olivine grains may have crystallized from more refractory melts in a condensation process [33] at a higher temperature than Ca-poor, Fe–Mn-rich olivine grains.

Similarly, thermal processing during chondrule formation may have been responsible for altering the compositions of some Mg-olivine grains. Relict grains in Ch-8 and Wel-12 have Fo and MnO contents intermediate to the high-$\Delta^{17}O$ grains in the host chondrules and other low-$\Delta^{17}O$ grains, and CaO contents more similar to the host grains (Fig. 5). This could be explained if the relict grains in Ch-8 and Wel-12 had chemical compositions originally more similar to those of other low-$\Delta^{17}O$ grains (with Fo > 92 mol.%, CaO > 0.35 wt.%, MnO < 0.05 wt.%), prior to chemical exchange with the host chondrule melts. Provided chemical exchange was rapid compared to isotopic exchange, the grains could have been chemically modified and still largely preserved their isotopic compositions (see Section 4.2).

4. Implications

4.1. Evolution of chondrule components and nebular oxygen

Some of our Type II chondrules (Wel-4, Wel-12, Ch-1, Ch-3, and Ch-8) contain relict forsterite (Fo_{99-100}) and Mg-rich olivine grains (Fo_{80-95}) that clearly
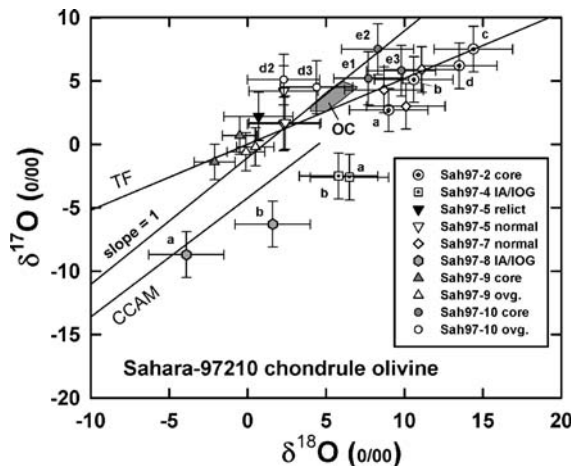
Fig. 4. Standard 3-isotope diagram for oxygen, showing the composition of olivine in Sahara-97210. IA/IOG = apparently fragmented Type I chondrules that resemble "isolated" grains; ovg. = overgrowth; other labels are the same as in Fig. 2.
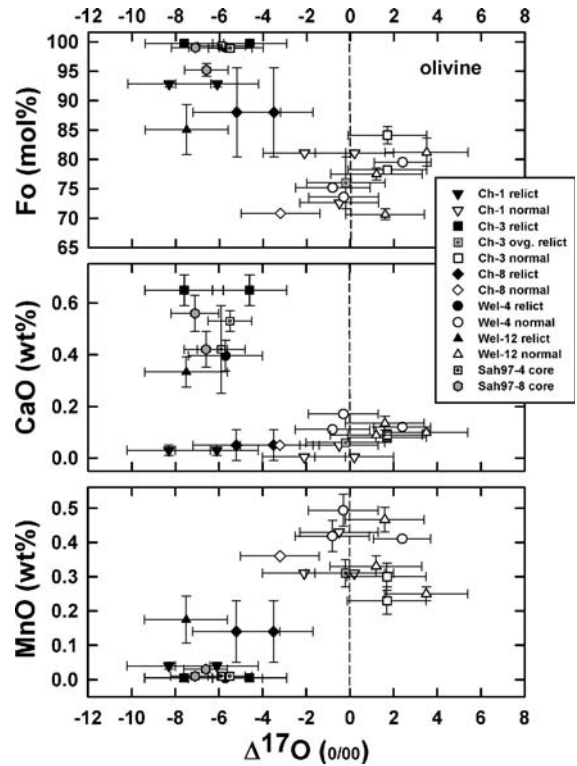
Fig. 5. Relationship between $\Delta^{17}O$ ($=\delta^{17}O - 0.52 \times \delta^{18}O$) determined by SIMS and chemical composition determined by EMPA for olivine in objects that contain some grains with significant deviations of oxygen-isotope compositions from the terrestrial fractionation line (dashed). Error bars are $\pm 1\sigma$ (internal precision for $\Delta^{17}O$, standard deviation for averaged chemical data). Ovg. = overgrowth.

formed in a different oxygen reservoir ($\Delta^{17}O \sim -8$ to -4‰) than their host chondrules ($\Delta^{17}O \sim -3$ to $+4$‰), similar to the ^{16}O-enriched reservoirs found in carbonaceous chondrites. The oxygen-isotopic and chemical compositions of the relict grains with low-$\Delta^{17}O$ in our study resemble the cores of isolated olivine grains that are probably fragmented chondrules (Sah97-4 and Sah97-8). We suggest that all these low-$\Delta^{17}O$ grains represent a single Mg-rich olivine population that formed in the same reservoir.

As relict grains pre-date normal olivine in the chondrules, our data imply that there was a temporal evolution of oxygen reservoirs to ^{16}O-depleted values in the source regions of ordinary chondrites. This conclusion is consistent with the inferences made for CAIs and chondrules in carbonaceous chondrites [10,15,18]. It is also consistent with inferences made for ferromagnesian chondrules in ordinary chondrites, as later-formed and more easily isotopically exchanged chondrule mesostases are depleted in ^{16}O compared to olivine and
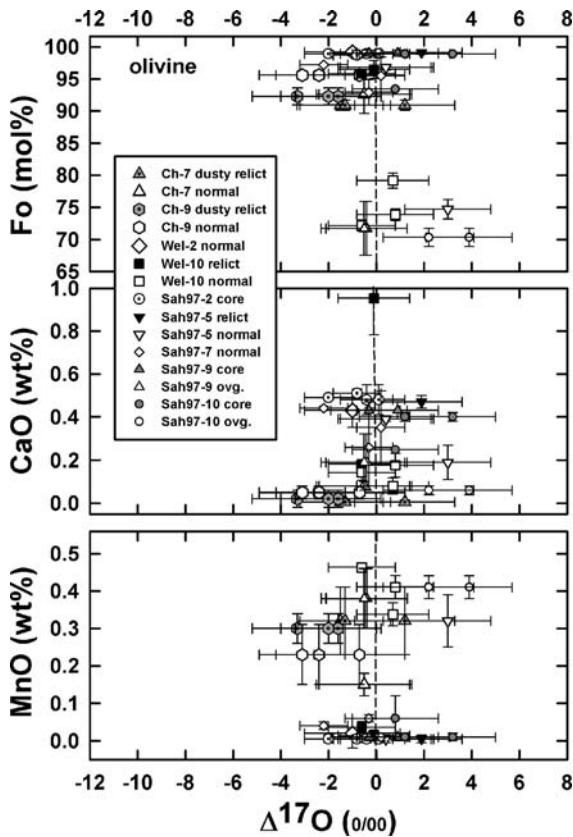
Fig. 6. Relationship between $\Delta^{17}O$ ($=\delta^{17}O - 0.52 \times \delta^{18}O$) determined by SIMS and chemical composition determined by EMPA for olivine in objects that do not contain grains with significant deviations of oxygen-isotope compositions from the terrestrial fractionation line (dashed). Error bars are $\pm 1\sigma$ (internal precision for $\Delta^{17}O$, standard deviation for averaged chemical data). Ovg. = overgrowth.

pyroxene [21], and as smaller (and thus more easily exchanged) chondrules in Chainpur are depleted in ^{16}O [19].

Although Bridges et al. [19,21] suggested that oxygen exchange in chondrules from ordinary chondrites may have occurred in the parent body, this cannot explain our results for olivine, as there is no evidence for any relationship between the isotopic composition of grains and their spatial location in chondrules. For example, grains with low $\Delta^{17}O$ values can occur immediately adjacent to chondrule edges (e.g., Wel-4, Ch-1, Ch-3) or near chondrule centers (e.g., Wel-12, Ch-8). The same is true for grains with high $\Delta^{17}O$ values. In our case, it is clear that isotopic evolution must reflect high-temperature processes associated with chondrule formation.

The low-$\Delta^{17}O$ population of Mg-rich olivine we identified is probably the same one as commonly found in carbonaceous chondrites. Our low-$\Delta^{17}O$ population resembles olivine grains in Type I chondrules from

carbonaceous chondrites in various ways, including similar oxygen-isotopic compositions [11,14,22,46,47], similar chemical compositions (Mg–Ca-rich and Fe–Mn-poor) [6,7,56], and similar grain sizes. The grains are also found in the same type of object (chondrules). However, in carbonaceous chondrites the low-$\Delta^{17}O$ grains are found mainly in Type I chondrules, whereas in ordinary chondrites the low-$\Delta^{17}O$ grains are found as relict grains in Type II chondrules. Isotopic and chemical compositions and grain sizes of our low-$\Delta^{17}O$ population are also similar to those of isolated forsterites found in carbonaceous chondrites [44,47,48,54]. Other similarities between these Mg-rich olivine grains from different chondrite groups are that they sometimes contain ferrous veinlets and inclusions of metal and glass. These grains in ordinary and carbonaceous chondrites formed in a similar oxygen reservoir, and their similar chemical compositions and grain sizes imply that they were thermally and physically processed in essentially the same way. These similarities among olivine grains establish a strong genetic link between the two chondrite classes [35,39].

However, other Mg-rich grains in our study formed in a different oxygen reservoir, indistinguishable from
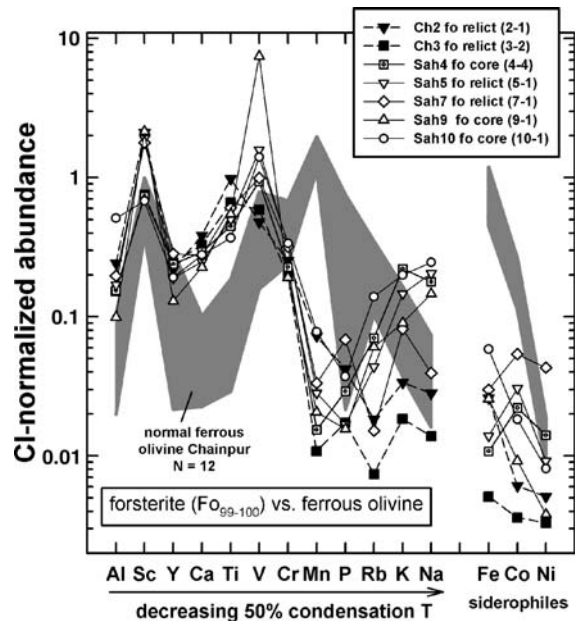

Fig. 7. CI chondrite-normalized abundances for various forsterite grains in Chainpur (Ch) and Sahara-97210 (Sah) compared to the compositional range for normal ferrous olivine in Chainpur (shaded, based on 12 analyses), determined by SIMS. From left to right, lithophile elements are arranged in order of decreasing 50% condensation temperatures, and siderophile elements are arranged in order of increasing siderophile tendency. The average CI chondrite abundances of Anders and Grevesse [67] were used for normalization.

that which produced the more ferrous olivine (Fo_{62-86}) in Type II host chondrules in Chainpur and Wells ($\Delta^{17}O \sim -3$ to $+4‰$). These include Mg-rich olivines (Fo_{97-100}) found in Type I chondrules with no relict grains (e.g., Wel-2), and in Type I chondrules in Sahara-97210 that contain ambiguous relict grains. Chondrules forming in this reservoir were recycled (remelted) under different conditions. For example, two dusty-olivine-bearing Chainpur chondrules (Ch-7 and Ch-9) were probably FeO-rich and reduced during remelting, producing the dusty relict grains (Fo_{89-94}), as well as zoned normal olivine (Fo_{87-97}) that crystallized from melt. Another chondrule, Wel-10, was evidently melted under oxidizing conditions, producing a Type II host chondrule with olivine more ferrous (Fo_{69-85}) than the Mg-rich olivine relict grains (Fo_{91-98}) it contains. In both cases, one involving Fe-reduction and the other Fe-oxidation, the oxygen reservoir did not significantly change between the time the relict grains originally formed and the time that the host chondrules were melted.

Most of our analyses correspond to the high-$\Delta^{17}O$ (-3 to $+4‰$) reservoir, and we suggest that this was the principal reservoir out of which chondrules in ordinary chondrites formed. The prevalence of this reservoir for ordinary chondrites is suggested by the bulk O-isotopic compositions of chondrules in ordinary chondrites ($\Delta^{17}O \sim +0.2$ to $+1.9‰$, [9]), which overlaps our high-$\Delta^{17}O$ reservoir, and by the many olivine and pyroxene grains in chondrules from various ordinary chondrites that isotopically resemble this bulk chondrule composition [19,21,35,36].

Altogether, the data we and others have obtained (see Introduction) are consistent with a model in which the nebular oxygen-isotopic reservoir changed to higher $\Delta^{17}O$ and less ^{16}O-enriched values with time, during an extended period of chondrule formation. Extended chondrule formation times (≥ 2 Ma) are implied based on ^{26}Al decay intervals [57–60]. We suggest that in an early stage, many Type I chondrules in carbonaceous chondrites were produced, as were forsteritic olivine grains that were later incorporated into ordinary chondrites. At later stages, which involved multiple melting episodes, both Type I and Type II chondrules were produced that were incorporated in ordinary chondrites.

The relationships between O-isotopic and chemical compositions of olivine in our data set (Sections 3.4 and 3.5) suggest that early heating events which produced refractory forsterites were relatively intense, whereas later events that produced Type II host chondrules were less intense. Later episodes of chondrule formation

occurred under a variety of conditions, including both intense heating to produce forsteritic and refractory olivine grains, and less intense heating to produce ferrous olivine. Although the data are consistent with a monotonic shift in $\Delta^{17}O$ for the reservoir to less negative values, it is not obvious that chondrule heating intensity changed with time in any systematic way. Early-formed forsteritic relicts produced by intense heating would have been preferentially preserved in ferrous Type II chondrule melts produced by less intense heating, because the grains would have had relatively high melting temperatures, inhibiting their dissolution. Indeed, as forsteritic olivine of similar composition and similar apparent heating intensity can have clearly different $\Delta^{17}O$, we conclude that there was no simple overall relationship between heating intensity and the isotopic composition of the reservoir (and hence time). Melting episodes characterized by variable heating intensity and variable redox conditions apparently extended throughout the chondrule-forming interval.

4.2. Heating timescales for relict grains and chondrules

Our data for oxygen-isotopic compositions in olivine grains in chondrules can be used to constrain chondrule heating timescales. Oxygen diffusion in olivine is very slow [38] compared to that in melt, whereas exchange between melt and surrounding gas is relatively rapid [61,70]. Thus, during remelting, one can model oxygen exchange between olivine grains and larger gas reservoirs by neglecting transport rates in the melt and considering only the properties of the grains themselves. We modeled oxygen exchange using the data of Ryerson et al. [38] for oxygen self-diffusion in olivine, assuming a reasonable value of fO_2 corresponding to 3 log units below the IW buffer [4], peak chondrule reheating temperatures of $\sim 1400–1850$ °C [3,62], and spherical olivine grains exchanging with an infinite surrounding reservoir. For this type of geometry, grains can be considered to have equilibrated if the duration of heating $t > 0.3 \times (a^2/D)$, where $a =$ grain radius and $D =$ diffusion coefficient ($\sim 4 \times 10^{-20}$ to $\sim 7 \times 10^{-17}$ m^2/s for temperatures ranging from 1400 to 1850 °C, respectively), and to have not significantly equilibrated if $t \leq 0.1 \times (a^2/D)$ [63]. The value of D depends only weakly on fO_2 ($D \propto fO_2^{0.2}$) [38], so the models are not especially sensitive to our assumed oxygen fugacity.

Our models assume a sufficient supply of oxygen from gas to the grains through chondrule melts, limited only by diffusion in olivine. However, if the supply of oxygen from the gas is limited, either by low gas

pressure [61] or by the kinetics of dissociation of gaseous species [71], the models will underestimate exchange times. The same is true if kinetic effects in the melt phase are important. Thus, our models provide a lower limit to exchange times for olivine grains and for chondrule heating timescales.

One type of calculation we performed was to evaluate the timescales required to preserve isotopically distinct relict grains. This applies to Mg-olivine relicts in Wel-12 ($a \sim 16$ µm for the Mg-rich core, ~ 74 µm for the entire grain), Wel-4 ($a \sim 75$ µm or ~ 115 µm), Ch-1 ($a \sim 27$ µm or ~ 43 µm), Ch-3 ($a \sim 45$ µm for the forsteritic core, which is isotopically distinct from the overgrowth), and Ch-8 ($a \sim 51$ or ~ 68 µm). Taking the smallest radii and maximum temperatures ($T = 1850$ °C) to obtain the shortest times to prevent equilibration, one finds heating times $t \sim 100$ h (Wel-12), ~ 500 h (Wel-4), ~ 200 h (Ch-1), ~ 700 h (Ch-3), and ~ 1000 h (Ch-8).

Considering that chondrules were molten for at most a few hours and perhaps ~ 1 h in each melting episode [3], these results imply that olivine would not isotopically equilibrate until after many dozens, and more probably hundreds or thousands, of remelting events. To get significant exchange evidently requires so much time, and temperatures so high, that the grains will almost certainly melt before they equilibrate. This conclusion is consistent with recent experimental studies [70]. Alternatively, the grains may have melted, but crystallized from distinct melt pockets that had not isotopically exchanged with the surrounding melt, if cooling rates were much faster than experiments imply. This possibility was suggested by Yurimoto and Wasson [13], who calculated cooling rates of $\sim 10^5–10^6$ °C/h for one chondrule containing a relict olivine. However, such rapid rates are inconsistent with monotonic zoning of normal olivine grains that appear to reflect fractional crystallization [3,4,62], and with models of chemical diffusion (Mg–Fe, Ca, Mn) between relict forsteritic cores and ferrous overgrowths, including the same grains studied here [64].

We also evaluated whether the two Mg-olivine relict grains in Wel-10, which have similar isotopic compositions to normal grains in the host chondrule, could have survived as grains from an inferred earlier episode of chondrule formation, but re-equilibrated with melts as a result of one or more heating events occurring in a different isotopic reservoir. Taking the radius of these relict grains to be ~ 35 µm and again the maximum temperature of 1850 °C so as to minimize the heating duration for equilibration, we calculate a heating time of ~ 1400 h. This result implies that the relict grains in Wel-10 would have had to crystallize from magnesian

melts after the reservoir composition had already changed.

The results of these models suggest that oxygen diffusion in olivine is so slow that it is practically impossible to equilibrate olivine by intracrystalline diffusion during chondrule melting episodes. Thus, the O-isotopic compositions of olivine grains are relatively insensitive to the thermal events that would have affected the grains during chondrule formation, and are instead an effective tracer of reservoir compositions. In contrast, we suggest that chemical exchange in olivine [64] occurred much faster than isotopic exchange, allowing the chemical compositions of some relict grains (e.g., the Mg-olivine relicts in Ch-8, Wel-12) to become modified during chondrule melting episodes (Section 3.5).

4.3. Mass fractionation during chondrule formation

Mass fractionation may have accompanied chondrule formation during intense heating events that resulted in vaporization. For oxygen isotopes, experiments show that it is difficult to produce mass fractionation in residual evaporated forsterite, but that evaporating forsterite melts can effectively record mass fractionation [65]. One of the two Chainpur chondrules analyzed containing relict dusty olivine (Ch-7) may have been mass-fractionated during chondrule formation, with the dusty olivine being lighter ($\delta^{18}O$ from -3.2 to $+1.3$‰, 3 analyses) than co-existing normal olivine ($\delta^{18}O$ from $+4.7$ to $+5.7$‰, 2 analyses). This difference in isotopic composition is consistent with evaporation in the melt out of which the normal olivine crystallized, as the later-formed normal olivine is isotopically heavier than the earlier (dusty) olivine along an approximate mass-fractionation trend (slope = $1/2$ in Fig. 3b, parallel to the TF line). If the experiments of Davis et al. [65] for a forsterite liquid are applicable, the magnitude of our measured shift for different grains in Ch-7 would imply between ~ 15 and 43% evaporation in the melt (taking into account the uncertainties in our oxygen values), with a best estimate of $\sim 27\%$ evaporation. The amount of evaporation experienced by a complex multicomponent liquid produced during partial remelting of the chondrule might be more or less than this value for a forsterite liquid. In the experiments of Davis et al. [65], this amount of mass fractionation was produced by vacuum evaporation at 1900 °C for tens of minutes. This might be too long to prevent the dusty olivine from melting [66], although coarse relict grains can survive close to their liquidus temperature for a few minutes [62,70,71], and the dusty olivine in Ch-7 is unusually

coarse. Besides Ch-7, there is the possibility of mass fractionation in object Sah97-10, which has forsteritic grain cores embedded in more ferrous olivine. The forsteritic cores appear to be mass-fractionated towards heavier values (with $\delta^{18}O \sim +7.7$ to $+9.8‰$, 3 analyses) than the ferrous grain overgrowths ($\delta^{18}O \sim +2.3$ to $+4.4‰$, 2 analyses) (Fig. 4). If this effect was produced during vaporization accompanying chondrule formation, it could be explained by re-equilibration of isotopically lighter gas with melt that crystallized to form the ferrous overgrowth olivine.

5. Conclusions

Relict and normal olivine grains in chondrules from three LL3.2-3.4 chondrites (Wells, Chainpur, Sahara-97210) have variable oxygen-isotopic and trace-element compositions. Significant grain-to-grain variations in isotopic compositions were found, which reflect mass-independent processes that correspond to the formation of olivine grains in different oxygen reservoirs, and which also sometimes appear to reflect mass-dependent processes associated with chondrule reprocessing events. Grains formed in at least two different oxygen reservoirs at different times. Some magnesian olivine grains (Fo_{85-100}), which are present both as relict grains in Type II host chondrules and as fragmented Type I chondrules, formed in a relatively ^{16}O-rich reservoir with low values of $\Delta^{17}O$ (~ -8 to $-4‰$). Olivine grains in this low-$\Delta^{17}O$ group are poor in MnO (< 0.2 wt.%) and usually are rich in CaO (0.3–0.65 wt.%). These grains probably formed relatively early from the same reservoir that produced Type I chondrules and "isolated" forsterite grains in carbonaceous chondrites. Other olivine grains, including those from Type I and Type II chondrules, as well as relict Mg-olivine and relict dusty grains, formed in a relatively ^{16}O-poor reservoir with high values of $\Delta^{17}O$ (~ -3 to $+4‰$). Olivine grains in this high-$\Delta^{17}O$ group have variable chemical compositions (Fo_{70-100}, MnO ~ 0–0.45 wt.%, CaO ~ 0–0.95 wt.%). These grains probably formed relatively late from the same reservoir that produced most Type I and II chondrules in ordinary chondrites. Chondrule formation in this second reservoir appears to have occurred under variable redox and heating conditions. One chondrule that contains an unusually large dusty olivine relict grain shows evidence of having experienced mass fractionation during remelting, involving perhaps ~ 15–43% evaporation from liquids. Another chondrule may have experienced partial re-equilibration with an isotopically-light oxygen gas reservoir during remelting

and vaporization. The trace element composition of forsterite (Fo_{99-100}) grains from both oxygen reservoirs are similar to one another and are chemically distinct from normal ferrous olivine grains, with the forsterites being enriched in refractory elements (Al, Sc, Y, Ca, Ti, V) and depleted in volatile elements (Cr, Mn, P, Rb, sometimes K and Na). This may indicate that forsteritic olivine grains experienced heating episodes that were higher in temperature or longer in duration than those which produced ferrous olivine grains. In general, whereas the chemical compositions of chondrule olivine grains appear to mainly reflect the conditions under which they formed, the oxygen-isotopic compositions of such grains are instead an effective tracer of reservoir compositions.

Appendix A. Supplementary data

Supplementary data associated with this article can be found, in the online version, at doi:10.1016/j.epsl.2007.02.037.

References

[1] J. Grossman, A.E. Rubin, H. Nagahara, E.A. King, Properties of chondrules, in: J.F. Kerridge, M.S. Matthews (Eds.), Meteorites and the Early Solar System, University of Arizona Press, Tucson, 1988, pp. 619–659.

[2] R.H. Hewins, Chondrules, Annu. Rev. Earth Planet. Sci. 25 (1997) 61–83.

[3] R.H. Hewins, H.C. Connolly, G.E. Lofgren, G. Libourel, Experimental constraints on chondrule formation, in: A.N. Krot, E.R.D. Scott, B. Reipurth (Eds.), Chondrites and the protoplanetary disk, Astronomical Society of the Pacific, San Francisco, 2005, pp. 286–316.

[4] R.H. Jones, J.N. Grossman, A.E. Rubin, Chemical, mineralogical and isotopic properties of chondrules: clues to their origin, in: A.N. Krot, E.R.D. Scott, B. Reipurth (Eds.), Chondrites and the Protoplanetary Disk, Astronomical Society of the Pacific, San Francisco, 2005, pp. 251–281.

[5] H.Y. McSween Jr., A. Kem Fronaberger, S.G. Driese, Ferromagnesian chondrules in carbonaceous chondrites, in: E.A. King (Ed.), Chondrules and Their Origins, Lunar and Planetary Institute, Houston, 1983, pp. 195–210.

[6] E.R.D. Scott, G.J. Taylor, Chondrules and other components in C, O, and E chondrites: similarities in their properties and origins, Proc. 14th Lunar Planet. Sci. Conf., 88, 1983, pp. B275–B286.

[7] E.R.D. Scott, A.N. Krot, Chondrites and their components, in: A.M. Davis (Ed.), Meteorites, Comets, and Planets, Treatise on Geochemistry, Elsevier, Amsterdam, 2005, pp. 143–200.

[8] R.N. Clayton, N. Onuma, Y. Ikeda, T.K. Mayeda, I.D. Hutcheon, E.J. Olsen, C. Molini-Velsko, Oxygen isotopic compositions of chondrules in Allende and ordinary chondrites, in: E.A. King (Ed.), Chondrules and their origins, Lunar and Planetary Institute, Houston, 1983, pp. 37–43.

[9] R.N. Clayton, T.K. Mayeda, J.N. Goswami, E.J. Olsen, Oxygen isotope studies of ordinary chondrites, Geochim. Cosmochim. Acta 55 (1991) 2317–2337.

[10] R.N. Clayton, Oxygen isotopes in meteorites, Annu. Rev. Earth Planet. Sci. 21 (1993) 115–149.

[11] R.H. Jones, J.M. Saxton, I.C. Lyon, G. Turner, Oxygen isotopes in chondrule olivine and isolated olivine grains from the CO3 chondrite Allan Hills A77307, Meteorit. Planet. Sci. 35 (2000) 849–857.

[12] R. Jones, L.A. Leshin, Y. Guan, Z.D. Sharp, T. Durakiewicz, A.J. Schilk, Oxygen isotope heterogeneity in chondrules from the Mokoia CV3 carbonaceous chondrite, Geochim. Cosmochim. Acta (2004) 3423–3438.

[13] H. Yurimoto, J.T. Wasson, Extremely rapid cooling of a carbonaceous–chondrite chondrule very ^{16}O-rich olivine and a ^{26}Mg-excess, Geochim. Cosmochim. Acta 66 (2002) 4355–4363.

[14] J.T. Wasson, A.E. Rubin, H. Yurimoto, Evidence in CO3.0 chondrules for a drift in the O isotopic composition of the solar nebula, Meteorit. Planet. Sci. 39 (2004) 1591–1598.

[15] T. Kunihiro, A.E. Rubin, K.D. McKeegan, J.T. Wasson, Oxygen-isotopic compositions of relict and host grains in chondrules in the Yamato 81020 CO3.0 chondrite, Geochim. Cosmochim. Acta 68 (2004) 3599–3606.

[16] R.N. Clayton, N. Onuma, L. Grossman, T. Mayeda, Distribution of the pre-solar component in Allende and other carbonaceous chondrites, Earth Planet. Sci. Lett. 34 (1977) 209–224.

[17] A.N. Krot, I.D. Hutcheon, H. Yurimoto, J.N. Cuzzi, K.D. McKeegan, E.R.D. Scott, G. Libourel, M. Chaussidon, J. Aléon, M.I. Petaev, Evolution of oxygen isotopic composition in the inner solar nebula, Astrophys. J. 622 (2005) 1333–1342.

[18] A.N. Krot, K.D. McKeegan, G.R. Huss, K. Liffman, S. Sahijpal, I.D. Hutcheon, G. Srinivasan, A. Bischoff, K. Keil, Aluminum–magnesium and oxygen isotope study of relict Ca–Al-rich inclusions in chondrules, Astrophys. J. 639 (2006) 1227–1237.

[19] J.C. Bridges, I.A. Franchi, R. Hutchison, A.S. Sexton, C.T. Pillinger, Correlated mineralogy, chemical compositions, oxygen isotopic compositions and size of chondrules, Earth Planet. Sci. Lett. 155 (1998) 183–196.

[20] S.S. Russell, G.J. MacPherson, L.A. Leshin, K.D. McKeegan, ^{16}O enrichments in aluminum-rich chondrules from ordinary chondrites, Earth Planet. Sci. Lett. 184 (2000) 57–74.

[21] J.C. Bridges, I.A. Franchi, A.S. Sexton, C.T. Pillinger, Mineralogical controls on the oxygen isotopic compositions of UOCs, Geochim. Cosmochim. Acta 63 (1999) 945–951.

[22] B.-G. Choi, K.D. McKeegan, L.A. Leshin, J.T. Wasson, Origin of magnetite in oxidized CV chondrites: in situ measurement of oxygen isotope compositions of Allende magnetite and olivine, Earth Planet. Sci. Lett. 146 (1997) 337–349.

[23] B.-G. Choi, K.D. McKeegan, A.N. Krot, J.T. Wasson, Extreme oxygen-isotope compositions in magnetite from unequilibrated ordinary chondrites, Nature 392 (1998) 577–579.

[24] E.D. Young, S.S. Russell, Oxygen reservoirs in the early solar nebula inferred from an Allende CAI, Science 282 (1998) 452–455.

[25] R.H. Jones, Relict grains in chondrules: evidence for chondrule recycling, in: R. Hewins, R. Jones, E. Scott (Eds.), Chondrules and the Protoplanetary Disk, Cambridge University Press, Cambridge, 1996, pp. 163–172.

[26] H. Nagahara, Evidence for secondary origin of chondrules, Nature 292 (1981) 135–136.

[27] E.R. Rambaldi, Relict grains in chondrules, Nature 293 (1981) 558–561.

[28] A. Kracher, E.R.D. Scott, K. Keil, Relict and other anomalous grains in chondrules: implications for chondrule formation, Proc. 14th Lunar Planet. Sci. Conf., vol. 89, 1984, pp. B559–B566.

[29] R.H. Jones, L.R. Danielson, A chondrule origin for dusty relict olivine in unequilibrated chondrites, Meteorit. Planet. Sci. 32 (1997) 753–760.

[30] H. Leroux, G. Libourel, L. Lemelle, F. Guyot, Experimental study and TEM characterization of dusty olivines in chondrites: evidence for formation by in situ reduction, Meteorit. Planet. Sci. 38 (2003) 81–94.

[31] J.T. Wasson, A.E. Rubin, Ubiquitous low-FeO relict grains in type II chondrules and limited overgrowths on phenocrysts following the final melting event, Geochim. Cosmochim. Acta 67 (2003) 2239–2250.

[32] A. Pack, H. Palme, Partitioning of Ca and Al between forsterite and silicate melt in dynamic systems with implications for the origin of Ca, Al-rich forsterites in primitive meteorites, Meteorit. Planet. Sci. 38 (2003) 1263–1281.

[33] A. Pack, H. Yurimoto, H. Palme, Petrographic and oxygen-isotopic study of refractory forsterites from R-chondrite Dar al Gani 013, unequilibrated ordinary and carbonaceous chondrites, Geochim. Cosmochim. Acta 68 (2004) 1135–1157.

[34] J.T. Wasson, Oxygen-isotopic evolution of the solar nebula, Rev. Geophys. 38 (2000) 491–512.

[35] J.M. Saxton, I.C. Lyon, G. Turner, Oxygen isotopes in forsterite grains from Julesburg and Allende: oxygen-16-rich material in an ordinary chondrite, Meteorit. Planet. Sci. 33 (1998) 1017–1027.

[36] D.W. Sears, I. Lyon, J. Saxton, G. Turner, The oxygen isotopic properties of olivines in the Semarkona ordinary chondrite, Meteorit. Planet. Sci. 33 (1998) 1029–1032.

[37] J. Koblitz, MetBase-Meteorite Data Retrieval Software, MetBase Version 6.0 for Windows, CD-ROM, 2003.

[38] F.J. Ryerson, W.B. Durham, D.J. Cherniak, W.A. Lanford, Oxygen diffusion in olivine: effect of oxygen fugacity and implications for creep, J. Geophys. Res. 94 (1989) 4105–4118.

[39] A. Ruzicka, H. Hiyagon, M. Prinz, L.A. Taylor, Forsteritic olivine grains in unequilibrated ordinary chondrites: additional evidence for a link between ordinary and carbonaceous chondrites, Lunar Planet. Sci., vol. XXXI, Lunar & Planetary Institute, 2000, #1312, (CD-ROM).

[40] A. Ruzicka, H. Hiyagon, C. Floss, Relict olivine, chondrule recycling, and evolution of oxygen reservoirs, Workshop on Oxygen in Asteroids and Meteorites, Lunar and Planetary Institute, 2005, #1422.

[41] A. Ruzicka, C. Floss, Relict forsterite and igneous olivine grains in Chainpur (LL3.5) chondrules: major- and trace-element evidence for vapor-fractionation and igneous partitioning, Lunar Planet Sci., vol. XXXIV, Lunar and Planetary Institute, 2003, #1243, (CD-ROM).

[42] A. Ruzicka, C. Floss, Forsterite and olivine in Sahara-97210 (LL3.2) and Chainpur (LL3.4) chondrules: compositional evolution and the influence of melting, Lunar Planet. Sci., vol. XXXV, Lunar and Planetary Institute, 2004, #1422, (CD-ROM).

[43] A. Ruzicka, C. Floss, M. Hutson, Trace-element compositions of normal, dusty, and clear olivine in Chainpur chondrules, Meteorit. Planet. Sci. 41 (2006) (#5266).

[44] I.M. Steele, Compositions and textures of relic forsterite in carbonaceous and unequilibrated ordinary chondrites, Geochim. Cosmochim. Acta 50 (1986) 1379–1395.

[45] H. Hiyagon, A. Hashimoto, ^{16}O excesses in olivine inclusions in Yamato-86009 and Murchison chondrites and their relation to CAIs, Science 283 (1999) 828–831.

[46] H. Hiyagon, In situ analysis of oxygen isotopes and Fe/Mg ratios in olivine using SIMS: preliminary results for an Allende chondrule, Antarct. Meteor. Res. 10 (1997) 249–274.

[47] I. Jabeen, H. Hiyagon, Oxygen isotopes in isolated and chondrule olivines of Murchison, Lunar Planet. Sci., vol. XXXIV, Lunar and Planetary Science Institute, 2003, #1551, (CD-ROM).

[48] L.A. Leshin, A.E. Rubin, K.D. McKeegan, The oxygen isotopic composition of olivine and pyroxene from CI chondrites, Geochim. Cosmochim. Acta 61 (1997) 835–845.

[49] E. Zinner, G. Crozaz, A method for the quantitative measurement of rare earth elements by ion microprobe, Int. J. Mass Spectrom. Ion Process. 69 (1986) 17–38.

[50] C.M. O'D. Alexander, Trace element distributions within ordinary chondrite chondrules: implications for chondrule formation conditions and precursors, Geochim. Cosmochim. Acta 58 (1994) 3451–3467.

[51] W. Hsu, Ion microprobe studies of the petrogenesis of enstatite chondrites and eucrites. Ph.D. Thesis. Washington University, 1995.

[52] E. Zinner, G. Crozaz, Ion probe determination of the abundances of all the rare earth elements in single mineral grains, in: A. Benninghoven, R.J. Colton, D.S. Simons, H.W. Werner (Eds.), Secondary Ion Mass Spectrometry, SIMS, vol. V, Springer-Verlag, New York, 1986, pp. 444–446.

[53] H. Hiyagon, N. Suguira, M. Kimura, A. Miyazaki, Refractory forsterites from Murchison (CM2) and Yamato 81020 (CO3.0) chondrites: cathodoluminescence, chemical compositions and oxygen isotopes, Workshop on Chondrites and Protoplanetary Disk, Lunar and Planetary Institute, 2004, #9032.

[54] S. Weinbruch, E.K. Zinner, A. El Goresy, I.M. Steele, H. Palme, Oxygen isotopic composition of individual olivine grains from the Allende meteorite, Geochim. Cosmochim. Acta 57 (1993) 2649–2661.

[55] B.A. Cohen, R.H. Hewins, C.M. O'D. Alexander, The formation of chondrules by open-system melting of nebular condensates, Geochim. Cosmochim. Acta 68 (2004) 1661–1675.

[56] A. Brearley, R. Jones, Chondritic meteorites, in: J.J. Papike (Ed.), Planetary Materials, Rev. Mineralogy, vol. 36, Mineralogical Society of America, Washington, D.C., 1998, pp. 3–1–3–398.

[57] N. Kita, H. Nagahara, S. Togashi, Y. Morishita, A short duration of chondrule formation in the solar nebula: evidence for ^{26}Al in Semarkona ferromagnesian chondrules, Geochim. Cosmochim. Acta 22 (2000) 3913–3922.

[58] G.R. Huss, G.J. MacPherson, G.J. Wasserburg, S.S. Russell, G. Srinivasan, Aluminum-26 in calcium-aluminum-rich inclusions and chondrules from unequilibrated ordinary chondrites, Meteorit. Planet. Sci. 36 (2001) 975–997.

[59] S. Mostefaoui, N.T. Kita, S. Togashi, S. Tachibana, H. Nagahara, Y. Morishita, The relative formation ages of ferromagnesian chondrules inferred from their initial aluminum-26/aluminum-27 ratios, Meteorit. Planet. Sci. 37 (2002) 421–438.

[60] K.D. McKeegan, A.M. Davis, Early solar system chronology, in: A.M. Davis (Ed.), Meteorites, Comets, and Planets, Treatise on Geochemistry, Elsevier, Amsterdam, 2005, pp. 431–460.

[61] Y. Yu, R.H. Hewins, R.N. Clayton, T.K. Mayeda, Experimental study of high temperature oxygen isotope exchange during chondrule formation, Geochim. Cosmochim. Acta 59 (1995) 2095–2104.

[62] R.H. Hewins, H.C. Connolly, Peak temperatures of flash-melted chondrules, in: R. Hewins, R. Jones, E. Scott (Eds.), Chondrules and the Protoplanetary Disk, Cambridge University Press, Cambridge, 1996, pp. 197–204.

[63] J. Crank, The mathematics of diffusion, 2nd Edition, Clarendon Press, Oxford, 1975, p. 414.

[64] S. Greeney, A. Ruzicka, Relict forsterite in chondrules: implications for cooling rates, Lunar Planet. Sci., vol. XXXV, Lunar and Planetary Institute, 2004, #1426, (CD-ROM).

[65] A.M. Davis, A. Hashimoto, R.N. Clayton, T.K. Mayeda, Isotope mass fractionation during evaporation of Mg_2SiO_4, Nature 347 (1990) 655–658.

[66] J.P. Greenwood, P.C. Hess, Congruent melting kinetics: constraints on chondrule formation, in: R. Hewins, R. Jones, E. Scott (Eds.), Chondrules and the Protoplanetary Disk, Cambridge University Press, Cambridge, 1996, pp. 205–211.

[67] E. Anders, N. Grevesse, Abundances of the elements: meteoritic and solar, Geochim. Cosmochim. Acta 53 (1989) 197–214.

[68] N.T. Kita, H. Nagahara, S. Tomomura, S. Tachibana, J.W. Valley, Systematic oxygen isotopic variations among chondrules from the least equilibrated ordinary chondrites: improved ion microprobe precision, Lunar Planet. Sci., vol. XXXVIII, Lunar and Planetary Institute, 2006, #1496, (CD-ROM).

[69] Meteoritical Bulletin Database. URL: http://tin.er.usgs.gov/meteor/metbull.php. Downloaded 2/13/2007.

[70] J. Boesenberg, M. Cosarinsky, K.D. McKeegan, M. Chaussidon, R.H. Hewins, An experimental study of Fe–Mg and oxygen-isotope exchange between relict olivine and chondrule melt, Lunar Planet. Sci., vol. XXXVIII, Lunar and Planetary Institute, 2007, #1621.

[71] J. Boesenberg, E.D. Young, K. Ziegler, R.H. Hewins, Evaporation and the absence of oxygen isotopic exchange between silicate melt and carbon monoxide gas at nebular pressures, Meteorit. Planet. Sci. 40 (2005) A22.